


Macrophage GSK3 β -deficiency inhibits the progression of hepatocellular carcinoma and enhances the sensitivity of anti-PD1 immunotherapy

Guangshun Sun,^{1,2} Hanyuan Liu,² Jie Zhao,¹ Jinyu Zhang,³ Tian Huang,¹ Guoqiang Sun,² Siqi Zhao ,² Zihao Zhang,¹ Hengsong Cao,¹ Dawei Rong,¹ Xiangyi Kong,¹ Qinghua Ji,⁴ Li Liu,^{5,6} Xuehao Wang,¹ Weiwei Tang ,¹ Yongxiang Xia ¹

To cite: Sun G, Liu H, Zhao J, *et al.* Macrophage GSK3 β -deficiency inhibits the progression of hepatocellular carcinoma and enhances the sensitivity of anti-PD1 immunotherapy. *Journal for ImmunoTherapy of Cancer* 2022;**10**:e005655. doi:10.1136/jitc-2022-005655

► Additional supplemental material is published online only. To view, please visit the journal online (<http://dx.doi.org/10.1136/jitc-2022-005655>).

GS, HL, JZ and JZ are joint first authors.

Accepted 01 December 2022



© Author(s) (or their employer(s)) 2022. Re-use permitted under CC BY-NC. No commercial re-use. See rights and permissions. Published by BMJ.

For numbered affiliations see end of article.

Correspondence to

Yongxiang Xia;
yx_xia@njmu.edu.cn

Weiwei Tang;
1243773473twww@sina.com

Xuehao Wang;
wangxh@njmu.edu.cn

Li Liu; jewtou@gmail.com

ABSTRACT

Background Glycogen synthase kinase 3 β (GSK3 β) was originally discovered to regulate glycogen synthesis and show a relationship to tumors. However, the biological functions of GSK3 β in tumor-associated macrophages (TAMs) in cancers including hepatocellular carcinoma (HCC) remain unclear.

Methods The enrichment of GSK3 β in tumor tissues was assessed by Gene Expression Omnibus (GEO) database. The in vitro and in vivo assays assisted in evaluating how GSK3 β in TAMs affected HCC in terms of proliferation, invasion and migration. Immunofluorescence was used to assess GSK3 β expression in TAMs in the anti-PD1 therapy non-responsive HCC group and the responsive group. Western blot and coimmunoprecipitation were performed to demonstrate the interaction between GSK3 β and PD-L1. We carried out in vivo experiments in a C57BL/6 mouse model of HCC established through subcutaneous injection.

Results GEO single-cell RNA sequencing data suggested that GSK3 β was highly enriched in TAMs of HCC. According to in vitro and in vivo experiments, reducing GSK3 β in TAMs inhibits the cancer cell proliferation, invasion, and migration. The immunofluorescence and immunohistochemistry results confirmed that the GSK3 β is significantly upregulated in TAMs of the anti-PD1 therapy non-responsive group in comparison with the responsive group. In vitro and in vivo experiments confirmed that reduced GSK3 β in TAMs are capable of enhancing the sensitivity of anti-PD1 immunotherapy for HCC by decreasing PD-L1 ubiquitination. Mass spectrometry results suggested that high expression of CD14⁺GSK3 β ⁺ in the peripheral blood mononuclear cell (PBMC) can predict non-responsive to anti-PD1 treatment. Moreover, escitalopram is confirmed to act as GSK3 β inhibitor that can increase the sensitivity of anti-PD1 immunotherapy for HCC.

Conclusions This study revealed that macrophage GSK3 β deficiency can inhibit the development of HCC by inhibiting the M2 phenotype and enhance the sensitivity of anti-PD1 immunotherapy for HCC by decreasing PD-L1 ubiquitination. The expression of CD14⁺GSK3 β ⁺ in PBMC can noninvasively predict anti-PD1 sensitivity in HCC patients, which provides novel strategies to predict anti-

WHAT IS ALREADY KNOWN ON THIS TOPIC

⇒ GSK3 β was originally discovered to regulate glycogen synthesis and show a relationship to tumors. But the biological functions of GSK3 β in tumor-associated macrophages (TAMs) in hepatocellular carcinoma (HCC) remain unclear.

WHAT THIS STUDY ADDS

⇒ This study revealed that macrophage GSK3 β deficiency can inhibit the HCC development, meanwhile enhancing the sensitivity exhibited by anti-PD1 immunotherapy for HCC. The CD14⁺GSK3 β ⁺ expression in peripheral blood mononuclear cell can non-invasively predict anti-PD1 sensitivity in HCC patients.

HOW THIS STUDY MIGHT AFFECT RESEARCH, PRACTICE OR POLICY

⇒ The study contributes to novel strategies to predict anti-PD1 sensitivity, increase anti-PD1 therapeutic effect, and bring new hope for HCC patients.

PD1 sensitivity, increase anti-PD1 therapeutic effect, and bring new hope for HCC patients.

INTRODUCTION

Hepatocellular carcinoma (HCC) takes up 90% of liver cancers, and it is the third major cause of death related to cancer. Nearly 80% of HCC patients do not conform to the indications for surgical resection because of late detection, distant metastasis, or poor organ function, and they can only be treated with drugs. The US Food and Drug Administration has identified two drugs, including multikinase and immune checkpoint inhibitors (ICIs), which can be adopted to treat advanced HCC. Existing studies have suggested that patients taking multikinase by oral only extended their median overall

survival by nearly 4 months.^{1–3} However, the advent of ICIs has opened new horizons for HCC treatment.

Cancer immunotherapy is that patients reactivate or strengthen their own immune system through a series of ways to precisely attack cancer cells for the treatment of cancer. Two of the first inhibitory immune checkpoints identified in the world are the cytotoxic T lymphocyte antigen 4 (CTLA4) and the programmed death 1 (PD1). Immune checkpoints including the above two can reduce T cell function or even turn off T cells through a series of cascade effects. The ICIs that have been developed so far, such as PD1 monoclonal antibody (mAb), can block the function of the above immune checkpoints, reactivate the antitumor effect of tumor-infiltrating T cells, and ultimately reshape immune function. Studies have demonstrated that approximately 50% of cancer patients (eg, melanoma, lung cancer, and clear cell renal cell carcinoma) benefit from ICIs such as ipilimumab (anti-CTLA4) and nivolumab (anti-PD1).^{4–6} It is encouraging that ICIs (eg, PD1 mAb) show therapeutic hope for patients with multiple malignancies (eg, HCC). Nevertheless, a small part of HCC patients significantly and durably respond to PD1 blockade.⁷ Accordingly, it is imperative to explore the mechanisms of primary resistance to anti-PD1 therapy in HCC patients.

Single-cell RNA-sequencing (scRNA-seq) deepens the understanding of cells-related behavior in a complicated tumor microenvironment, particularly analyzing cell populations at individual cell level.^{8,9} Glycogen synthase kinase 3 β (GSK3 β) was found to be highly enriched in tumor-associated macrophages (TAMs) based on Gene Expression Omnibus (GEO) scRNA-seq data. HCC biopsy specimens of responsive and non-responsive to anti-PD1 treatment were validated using immunofluorescence. We were fortunate to find that the GSK3 β was significantly upregulated in TAMs from the non-responsive group in comparison with the responsive group. GSK3 β is a relatively traditional protein kinase. It is widely expressed in various tissues of the body and can remarkably help to regulate various cellular functions. GSK3 β is inhibited under normal conditions, whereas it can be abnormally activated under abnormal stress conditions to participate in processes (eg, cell death or proliferation), which is dependent on its subcellular localization and specific partners. Existing research has suggested that GSK3 β can be abnormally activated in inflammation and tumors, and it plays a certain role in the dysregulation of adult stem cells.^{10,11} However, GSK3 β in TAMs from HCC has been rarely investigated. Thus, this study will focus on clarifying the function and mechanism of GSK3 β in TAMs of HCC and how it mediates anti-PD1 primary resistance.

Materials and methods

GEO data analysis

We acquire data from GEO database (GSE151530 and GSE164522) and studied the difference of GSK3 β mRNA expressing in TAMs. We screened single cells for

conducting downstream analysis in accordance with the criteria of unique molecular identifier (UMI) counts in the range of 3000 and 40,000; and mitochondrial percentages <10% of the total UMI count. The standardized gene expression scale (in UMI) was converted to LOG2 (UMI+1).

Cases and tissue specimen collection

After the removal from the body, the overall samples were acquired. Authoritative clinicians took charge of confirming and classifying the tumor specimens involved in the article.

Cancer cell culture

The THP-1 cells, mice HCC cells (Hep1-6) as well as human HCC cells (LM3 and YY8103) were offered by the Cell Bank of Type Culture Collection. RPMI 1640 medium (BI, USA) was added with 10% FBS (Fetal Bovine Serum), which was used to culture the THP-1 cells, Hep1-6 cells, LM3 cells and YY8103 cells. 1.8 μ L/500 mL β -Mercaptoethanol (Gibco, USA) was added in the process of cultivation of THP-1. The culture conditions were 37°C, 5% CO₂ chamber.

Induction of TAMs in HCC

The 100 nM Phorbol-12-myristate-13-acetate were employed for inducing THP-1 differentiation into M0 macrophages after 2 days, during which the cells changed from a suspended state to an adherent state. In the process of culturing M0 macrophages, the medium supernatant of LM3 or YY8103 cells was added to mimic the HCC tumor microenvironment to stimulate the differentiation of M0 cells into TAMs. After 48–72 hours, when the cells grow antennae, it means that we have obtained the key cells of this experiment: HCC tumor-associated-macrophages. In the process of differentiation from M0 cells to TAM cells, we divided them into different groups, adding PBS (Phosphate Buffered Saline), GSK3 β inhibitor (MCE, USA) and escitalopram (GLP BIO, USA) respectively, to observe the difference of TAMs obtained in different groups. After obtaining different groups of TAMs, continue to culture cells and collect TAM medium supernatant from different groups (PBS group, GSK3 β inhibitor group, escitalopram group) for following experiments (online supplemental figure S1E).

Cell proliferation assay

Fifty per cent TAM-conditioned medium was used to culture LM3 and YY8103 cells for 24 hours before following experiments with cancer cells. The 50% TAM-conditioned medium contains 50% normal cancer cell culture medium (RPMI 1640 medium with 10% FBS) and 50% TAM culture supernatant from different groups collected in the above TAMs culture process, which were PBS group, GSK3 β inhibitor group, and escitalopram group. For detecting CCK-8, we seeded 10³ tumor cells into 96-well plates. Next, the above cells were administered with 10 μ L of CCK-8 solution for 0, 24, 48, and 72 hours, respectively. Using a microplate reading

element as per the manufacturer's protocol, we examined the cell absorbance at the respective time points of 450 nm. A 5-ethynyl-2'-deoxyuridine (EdU) assay served for evaluating cell proliferation based on the Cell-Light EdU DNA Cell Proliferation Kit. 5×10^4 cancer cells were placed in 24-well plates and cells underwent the incubation of fixed cell lines and 4% paraformaldehyde and 50 Easy for 2H/L EdU solution for 24 hours. We have kept Apollo Stain and Hearst Stamps separate with the manufacturer's approval. An Olympus FSX100 microscope assisted in obtaining as well as calculating EdU cell lines.

TRANSWELL ASSAY

LM3 and YY8103 cells were cultured with 50% TAM-conditioned medium for 48 hours. The 50% TAM-conditioned medium contains 50% normal cancer cell culture medium (RPMI 1640 medium with 10% FBS) and 50% TAM culture supernatant from different groups collected in the above TAM culture process, which were PBS group, GSK3 β inhibitor group, and escitalopram group. Next, we seeded YY8103 and LM3 cells in the chamber and 200 μ L of RPMI 1640 medium free of serum was added for their survival. For the invasion efficiency test, we scattered the matrigel mixture in the transwell chamber. Matrigel mixtures are not used for migration efficiency measurements. Both cells were induced into the bottom chamber with RPMI 1640 medium and 10% FBS as inducers. Following 48 hours of incubation, the upper chamber underwent fixing treatment in formaldehyde together with 15 min of crystal violet staining. The cells were photographed in three fields of view for visualization.

Scratch wound experiment

LM3 and YY8103 cells were cultured with 50% TAM-conditioned medium for 48 hours. The 50% TAM-conditioned medium contains 50% normal cancer cell culture medium with 10% FBS and 50% TAM culture supernatant from different groups collected in the above TAM culture process, which were PBS group, GSK3 β inhibitor group, and escitalopram group. Each well of a six-well plate was inoculated with 200,000–300,000 cells and thoroughly mixed during inoculation. When the confluence of cells reached 100%, the cell culture medium was aspirated. Floating cells were carefully washed twice with 1 \times PBS (Gibco, USA). Using a 20 μ L pipetting gun tip, make three horizontal lines for each hole. The floating cells were carefully cleaned with 1 \times PBS. After the background was clean, 1 mL of 1 \times PBS was added to each well and the scratches were photographed under a microscope at 4 \times low power. On day 0, day 1, and day 2, the scratches in each well were photographed under a microscope at 4 \times low power. Record and analyze pictures.

Quantitative reverse transcription PCR

TRIzol reagent assisted in isolating total RNA of TAM cells as per the manufacturer's instruction. The reverse

transcription kit helped to synthesize cDNA into mRNA. Online supplemental table S1 shows all primer sequences. GAPDH served for normalizing mRNA expression levels.

Immunofluorescence and immunohistochemistry

For the immunofluorescence assay, in the first step, we fixed cells using 4% paraformaldehyde for 20 min at room temperature, followed by 5 min of permeation using 0.05% Triton X-100 at room temperature. The samples were then blocked overnight in 2% BSA in PBS at room temperature and incubated with CD163 (Abcam, UK) and GSK3 β (Abcam, UK) specific antibodies at 4 $^{\circ}$ C, followed by conjugation with Alexa Fluorite or HRP at room temperature. The combined secondary antibody (Abcam, UK) was incubated with temperature for 1 hour. Nuclei were restained using DAPI (Sigma-Aldrich, USA). A laser scanning confocal microscope (Zeiss, Germany) was employed for obtaining images.

For immunohistochemistry, the paraffin-embedded sections underwent dewaxing and rehydration treatment. Three per cent hydrogen peroxide blocked the peroxidase activity. Sections received one night of incubation using primary antibodies (PD1, CD8, Ki67, PD1, and PD-L1; Abcam, UK) at 4 $^{\circ}$ C. Next, the biotinylated secondary antibody was employed for treating tissue sections. Subsequently, Finally, streptavidin-horseradish peroxidase complex was selected to incubate the sections.

Western blotting and coimmunoprecipitation

We extracted proteins from cells using RIPA buffer solution (Sigma-Aldrich, USA), and the extracted proteins were lysed by using SDS-polyacrylamide gels, followed by being transferred to PVDF membranes. Primary antibodies against GSK3 β , GSK3 β (ser9), PD-L1 were employed (Abcam, UK). GAPDH was assigned into the control. A peroxidase-conjugated secondary antibody employed used with enhanced chemiluminescence. The HA-ubiquitin was incubated with the total protein, and the western blotting assisted in analyzing the products after incubation.

The 293T cells were cotransfected with corresponding plasmids. After 48 hours, the transfected cells were collected, added with 0.4 mL RIPA lysis buffer, and the cells were thoroughly mixed. Lysis was carried out at 4 $^{\circ}$ C for half an hour. After lysis, centrifugation was performed at 12 000 rpm for half an hour at 4 $^{\circ}$ C. The supernatant after centrifugation was collected for the next step. The supernatant was incubated with anti-FLAG or anti-HA magnetic beads. After completion of incubation, it was washed three times, followed by one night of incubation at 4 $^{\circ}$ C. Before immunoprecipitation, the samples were washed three times and boiled in 5 \times SDS loading buffer. The buffer contained 0.2% (w/v) bromophenol blue, 20% (v/v) glycerol, 100 mM Tris-HCl (pH 6.8), 10% (w/v) SDS, and 1% (v/v) 2-mercaptoethanol. Then routine electrophoresis, membrane transformation, blocking and

corresponding antibody incubation were performed. Finally, the membrane was visualized and the data were analyzed.

Mice model

The animal experiment gained approval of the animal management committee of The First Affiliated Hospital of Nanjing Medical University and the approved ID number is 2021-SRFA-197. All experiment procedures and animal caring were following the institutional ethics directions for animals-relevant experimental processes. C57BL/6, GSK3 β ^{fl/fl} and Lyz2-Cre mice came from Gem Pharmatech Co., Ltd. Hybridization of GSK3 β ^{fl/fl} mice and Lyz2-Cre mice produced myeloid-specific knockout mice. We set mice that possessed Lyz2-specific deletion of GSK3 β as CKO mice, and GSK3 β ^{fl/fl} mice as the controls. PCR helped to analyze the genomic DNA from mouse tails.

Myeloid-specific knockout mice: The subcutaneous injection of Hep1-6 cells was made into GSK3 β ^{fl/fl} C57BL/6 mice (n=5) and GSK3 β ^{fl/fl} Lyz2^{cre/+} C57BL/6 mice (n=5), respectively. Tumor model mice with carcinoma transplantation fell into four groups, GSK3 β ^{fl/fl}, GSK3 β ^{fl/fl} Lyz2^{cre/+}, GSK3 β ^{fl/fl}+anti-PD1 (bioxcell,USA), GSK3 β ^{fl/fl} Lyz2^{cre/+}+anti-PD1, and each group had five mice. Specifically, 6.6 mg/kg anti-PD1 were intraperitoneally injected into mice on the eighth day, and once every 4 days subsequently.

Wild-type mice experiment (GSK3 β inhibitor): The subcutaneous injection of Hep1-6 cells was made into C57BL/6 mice. Tumor model mice with carcinoma transplantation fell into four groups, PBS, GSK3 β inhibitor, anti-PD1, GSK3 β inhibitor+anti-PD1, and each group had five mice. Specifically, GSK3 β inhibitor was intraperitoneal injected with 10 mg/kg on the first day and once per 4 days later; 6.6 mg/kg anti-PD1 were intraperitoneally injected into mice on the eighth day, and once every 4 days subsequently.

Wild-type mice experiment (escitalopram): The subcutaneous injection of Hep1-6 cells was made into C57BL/6 mice. Tumor model mice with carcinoma transplantation fell into four groups, PBS, escitalopram, anti-PD1, escitalopram+anti-PD1, and each group had five mice. To be Specifically, escitalopram was intraperitoneal injected with 10 mg/kg on the first day and once per 4 days thereafter; 6.6 mg/kg anti-PD1 were intraperitoneally injected into mice on the eighth day, and once every 4 days later.

The basic condition of the mice was observed every day prior to and following the experiment. Vernier calipers served for measuring the long diameters a (mm) and short diameters b (mm) of tumors on the body surface, and the tumor volume was calculated according to $V = ab^2/2$. The tumor growth curve was finally generated by measuring the tumor volume every 4 days. At day 20, mice were sacrificed and tumor mass data were obtained for further analysis.

Mass spectrometry

The tissue samples were from GSK3 β ^{fl/fl}, GSK3 β ^{fl/fl} Lyz2^{cre/+} C57BL/6 mice. Nine anti-PD1 pretreatment peripheral blood mononuclear cell (PBMC) samples from HCC patients' blood samples were examined through mass spectrometry. CyTOF staining steps comprised 194Pt staining → Fc block → surface antibody staining → overnight DNA staining (191/193Ir) → intracellular antibody staining → collecting data on the computer. A two-step method was used for data analysis. First, single, viable and intact CD45+ immune cells were obtained by FlowJo pretreatment. Then, the X-shift algorithm was used to cluster cell subpopulations, manually annotate cell subpopulations, visualize TSNE dimensionality reduction, and perform statistical analysis.

FLOW CYTOMETRY

Isolated PBMCS from 19 HCC patients received staining treatment by using the antibodies including PE anti-human CD14 and AF647 anti-human GSK3 β . The flow cytometry (BD FACS Canto II, USA) helped to analyze the molecular phenotypes regarding the peripheral blood leucocytes. The FlowJo V.10 (Tree Star, USA) software analyzed the samples.

Statistical analysis

GraphPad Prism V.8.0 assisted in the statistical analysis, and a $p < 0.05$ indicated a difference achieving statistical significance. Independent t-tests were used for comparing continuous variables between the two groups, whereas one-way analysis of variance served for comparing multiple groups.

RESULTS

GSK3 β was enriched in TAMs of tumors based on scRNA-seq

The data originated from GEO database (GSE151530 and GSE164522), and the difference of GSK3 β mRNA expressing in TAMs was examined. GSE151530 results indicated that 46 HCC tumor samples were enrolled in scRNA-seq. A total of 6 cell clusters, comprising B lymphocytes (B cells), tumor-associated fibroblasts (CAFs), malignant cells, T cells, and TAM, thymic epithelial cells, were found according to the classification definition of specific gene markers (figure 1A,B). For example, the TAM cluster is capable of specifically expressing GSK3 β (figure 1B). The point diagram showed that GSK3 β was highly enriched in TAMs (figure 1C). In addition, GSE164522 comprised 10 colorectal cancer liver metastasis patients for scRNA-seq. The results showed that 12 cell clusters were confirmed, which comprised B cells, CD4⁺ T cells, CD8⁺ T cell, DC, natural killer (NK) cells, macrophages, ILC3, MAST, Monocyte, gdT, NKT, CD45-cells based on specific gene markers (figure 1D,E). The violin plot showed that GSK3 β was highly enriched in TAMs (figure 1F). All the above outcomes suggested that GSK3 β may play a vital role in TAMs of HCC.

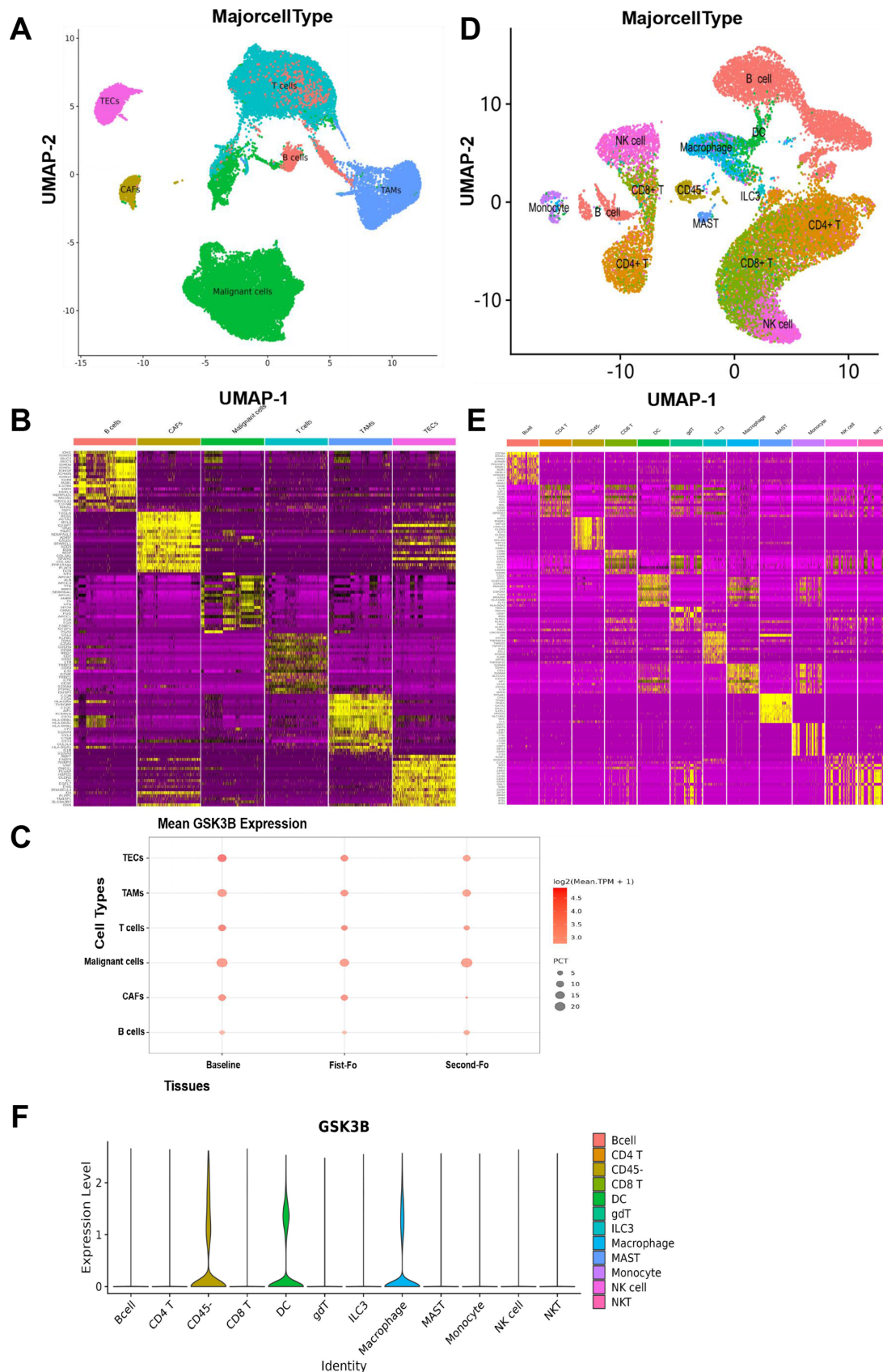


Figure 1 GSK3 β was enriched in TAMs of tumors based on scRNA-seq. (A, B) UMAP map identifies 6 cell clusters that define the classification of specific gene signatures, including B cells, CAFs, malignant cells, T cells, TAMs, TECs based on GSE151530. (C) The point diagram showing expression of GSK3 β in TAMs. Baselines, first, second indicates specimens collected at different time points. (D, E) UMAP map identifies 12 cell clusters based on GSE164522. (F) The violin plot showing expression of GSK3 β in TAMs. TAMs, tumor-associated macrophages; TECs, thymic epithelial cells.

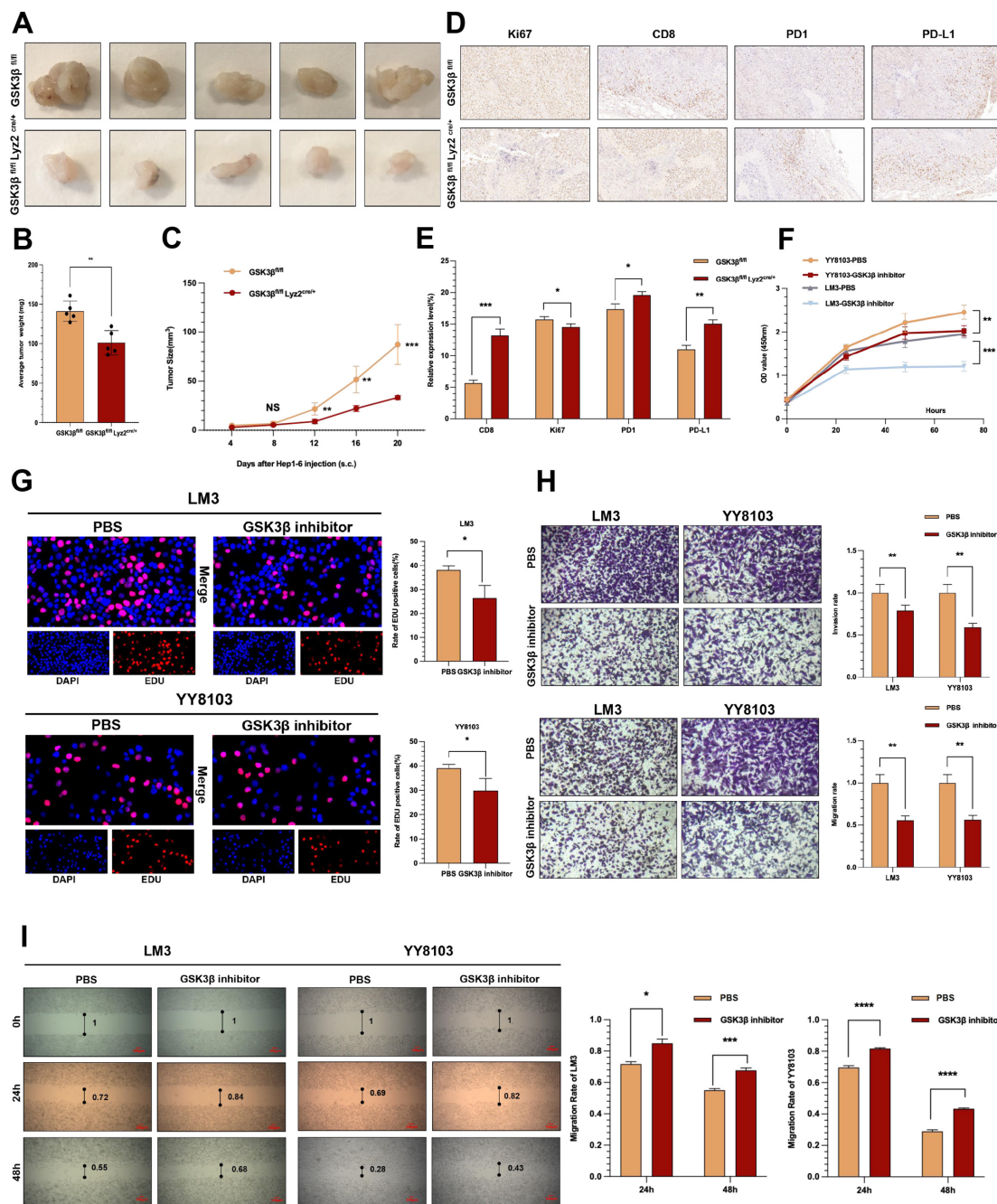


Figure 2 Macrophage GSK3 β deficiency inhibited the progression of HCC. (A) Images of subcutaneous tumors in each group (GSK3 β ^{fl/fl} Lyz2^{cre/+}, GSK3 β ^{fl/fl}). (B, C) Weight and volume analysis of subcutaneous tumors in the respective groups. (D, E) Immunohistochemistry results of CD8, Ki67, PD-L1 and PD1 expression in the respective groups. (F) The growth curves of HCC cells were plotted after cultured with TAMs added GSK3 β inhibitor based on CCK-8 assays. (G) EdU assays were performed to assess cell proliferation of LM3 and YY8103 cell lines cultured with TAM added GSK3 β inhibitor. (H) Transwell experiment was adopted to assess cell invasion and migration of HCC cells incubated with TAM added GSK3 β inhibitor. (I) Wound healing assays were used to assess cell migration of HCC cells after cultured with TAM added GSK3 β inhibitor. * $p < 0.05$, ** $p < 0.01$, *** $p < 0.001$, **** $p < 0.0001$. HCC, hepatocellular carcinoma; TAM, tumor-associated macrophage.

Macrophage GSK3 β deficiency inhibited the progression of HCC

Based on the above results, the role played by GSK3 β expression changes in TAMs in HCC tumors was investigated. Hep1-6 cells were injected in GSK3 β ^{fl/fl} and GSK3 β ^{fl/fl} Lyz2^{cre/+} C57BL/6 mice to investigate the role played by GSK3 β in TAM on tumors. GSK3 β ^{fl/fl} mice and

GSK3 β ^{fl/fl} Lyz2^{cre/+} mice presented more rapid and slower subcutaneous tumor growth, respectively (figure 2A). On the 20th day, we sacrificed the mice, obtaining their subcutaneous tumors. The volume and weight of subcutaneous tumors in GSK3 β ^{fl/fl} Lyz2^{cre/+} mice were significantly smaller than those in GSK3 β ^{fl/fl} mice (figure 2B,C), suggesting that GSK3 β knockout in TAMs remarkably

suppresses HC tumor occurrence and development. According to immunohistochemistry results, compared with the GSK3 β ^{fl/fl} mice group, GSK3 β ^{fl/fl} Lyz2^{cre/+} group exhibited obviously upregulated PD1, PD-L1 and CD8 expressions, and downregulated Ki67 expression (figure 2D,E).

For further confirming the anticancer role played by GSK3 β in TAMs in HCC, we attempted to induced normal TAM and inhibited GSK3 β activity in TAMs. We stimulated HCC cells with 50% TAM-conditioned medium from different groups and found that GSK3 β inhibitor group in TAMs significantly reduced the proliferation of LM3 and YY8103 cells than the PBS group (figure 2F,G). Transwell assay and scratch assay indicated that GSK3 β inhibitor group could obviously hinder the invasion and migration functions of LM3 and YY8103 cells (figure 2H,I). The above results demonstrated that inhibiting GSK3 β in TAMs can inhibit human HCC cells in terms of the proliferation, the invasion, and the migration.

GSK3 β deficiency in TAMs inhibited NF- κ B pathway to mediate antitumor activity

Quantitative reverse transcription PCR (qRT-PCR) served for detecting the expression of makers related to TAMs after treatment with GSK3 β inhibitor or PBS. The results indicated the considerably lower CD206, CD163 and ARG1 expressions in GSK3 β inhibitor group relative to the control group (online supplemental figure S1A,B). For confirming the mechanism of GSK3 β in cancer promotion mediated by TAM, we reviewed the literature and guessed that it may be related to NF- κ B signaling pathway.¹² We found that P-P65 was substantially reduced in the GSK3 β inhibitor TAMs while P65 showed no difference (online supplemental figure S1C,D). To examine the function of GSK3 β /NF- κ B pathway in TAMs, we paid attention to examining the underlying regulatory impact of GSK3 β on the direct NF- κ B-targeted genes including STAT1, CCL5, IL6, CSF2 by qRT-PCR array in vitro.¹² The result revealed that the STAT1, CCL5, IL6, CSF2 decreased in GSK3 β inhibitor group (online supplemental figure S1A,B). In addition, we added the NF- κ B inhibitor, meanwhile examining the potential expression of the markers. The result revealed the considerably lower CD206, CD163 and ARG1 expressions relative to the control group, which was consistent with GSK3 β inhibitor results (online supplemental figure S1A,B). The above evidence suggested GSK3 β deficiency in TAMs inhibited NF- κ B pathway to mediate antitumor activity.

GSK3 β was enriched in TAMs of tumors in the primary resistance of anti-PD1 immunotherapy for HCC

Based on our group's previous studies on GSK3 β and liver immune activation,¹³⁻¹⁶ we wondered if GSK3 β mediated primary resistance to the anti-PD1 treatment in HCC. We took six puncture samples non-responsive to the anti-PD1 treatment and five puncture samples responsive to the anti-PD1 treatment for immunofluorescence detection, and the results showed that CD163⁺ GSK3 β ⁺ expression

was higher in anti-PD1 non-responder group in comparison with responder group (figure 3A-C). The above evidence indicated that GSK3 β in TAMs was upregulated in non-responders of anti-PD1 therapy in HCC. For more deeply verifying as well as analyzing the conclusions obtained so far. We collected five human HCC tumor specimens and performed immunohistochemical experiments to analyze the expression of GSK3 β and PD-L1 proteins in these specimens. As revealed from the results, the GSK3 β expression was negatively related to PD-L1 in HCC tissues. Patients with relatively high GSK3 β expression possessed a lower PD-L1 expression (figure 3D-F). Above experiments revealed that increased GSK3 β expression in TAM was associated with the primary resistance of anti-PD1 immunotherapy for HCC.

Macrophage GSK3 β deficiency enhanced the sensitivity of anti-PD1 immunotherapy for HCC by decreasing PD-L1 ubiquitination

Since GSK3 β mediates primary anti-PD1 resistance, what is the relationship between GSK3 β and PD-L1? GSK3 β induces the PD-L1 proteasomal degradation dependent of phosphorylation in cancer cells, thereby primarily regulating the tumor immunity.¹⁷ On that basis, a hypothesis was proposed that GSK3 β might play a similar regulatory role on PD-L1 ascent in TAM cells. Western blot verified that the GSK3 β inhibitor in TAMs elevated PD-L1 expression (online supplemental figure S2A). For verifying the association of GSK3 β with PD-L1, we performed co-immunoprecipitation (Co-IP) experiments. After transfection with GSK3 β plasmid, the ubiquitination level of PD-L1 was on the rise, while the expression of PD-L1 decreased (figure 4A, online supplemental figure S2B). Also, GSK3 β and PD-L1 interacted with each other through Co-IP (figure 4B). Finally, we observed colocalization of GSK3 β and PD-L1 through immunofluorescence experiments (figure 4C). These results verified the interaction of GSK3 β and PD-L1. In addition, TISIDB database demonstrated the negative relevance of GSK3 β expression to the expressions of CD8⁺ T cells, PD1, TIGIT, and CTLA4 in 373 HCC samples (online supplemental figure S3). All the above evidence suggested that increased GSK3 β may inhibit PD-L1 expression in HCC, thereby causing primary resistance of anti-PD1 therapy.

To explore the changes of the tumor immune micro-environment of HCC in GSK3 β deficiency from macrophages, we detected two tumor samples from GSK3 β ^{fl/fl} and GSK3 β ^{fl/fl} Lyz2^{cre/+} mice through mass spectrometry, respectively. We dissociated tumor specimens from both groups, meanwhile recycling single intact CD45⁺ immune cells with normal activity from the cell masses. All samples showed clustering and subgroup annotation of CD45⁺ immune cells. A total of 31 cell clusters were obtained, with each defined by its specific marker (online supplemental figure S4, figure 4D,F). After comparing the numbers of the two groups, we found that the relative proportions of some cell clusters, such as M2 macrophages, MDSC and treg, showed a downward trend in the GSK3 β ^{fl/fl} Lyz2

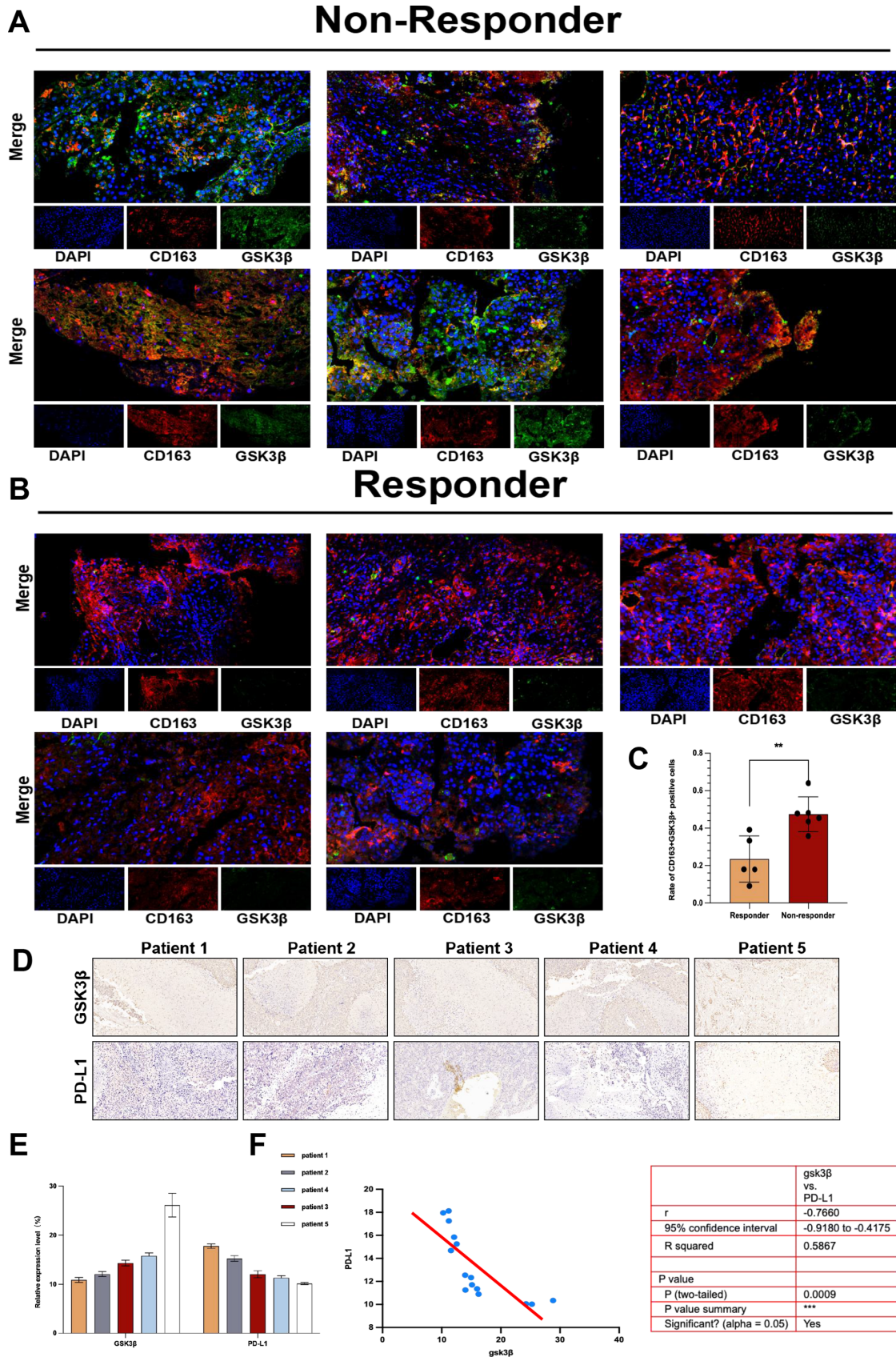


Figure 3 GSK3 β was enriched in TAMs of tumors in the primary resistance of anti-PD1 immunotherapy for HCC. (A–C) The immunofluorescence was used to verify the different CD163+GSK3 β +expression in TAMs between non-responder to anti-PD1 treatment group and responder group. (D–F) Immunohistochemistry results of GSK3 β and PD-L1 expression in the non-responder to anti-PD1 treatment group and responder group. ** $p < 0.01$. HCC, hepatocellular carcinoma; TAMs, tumor-associated macrophages.

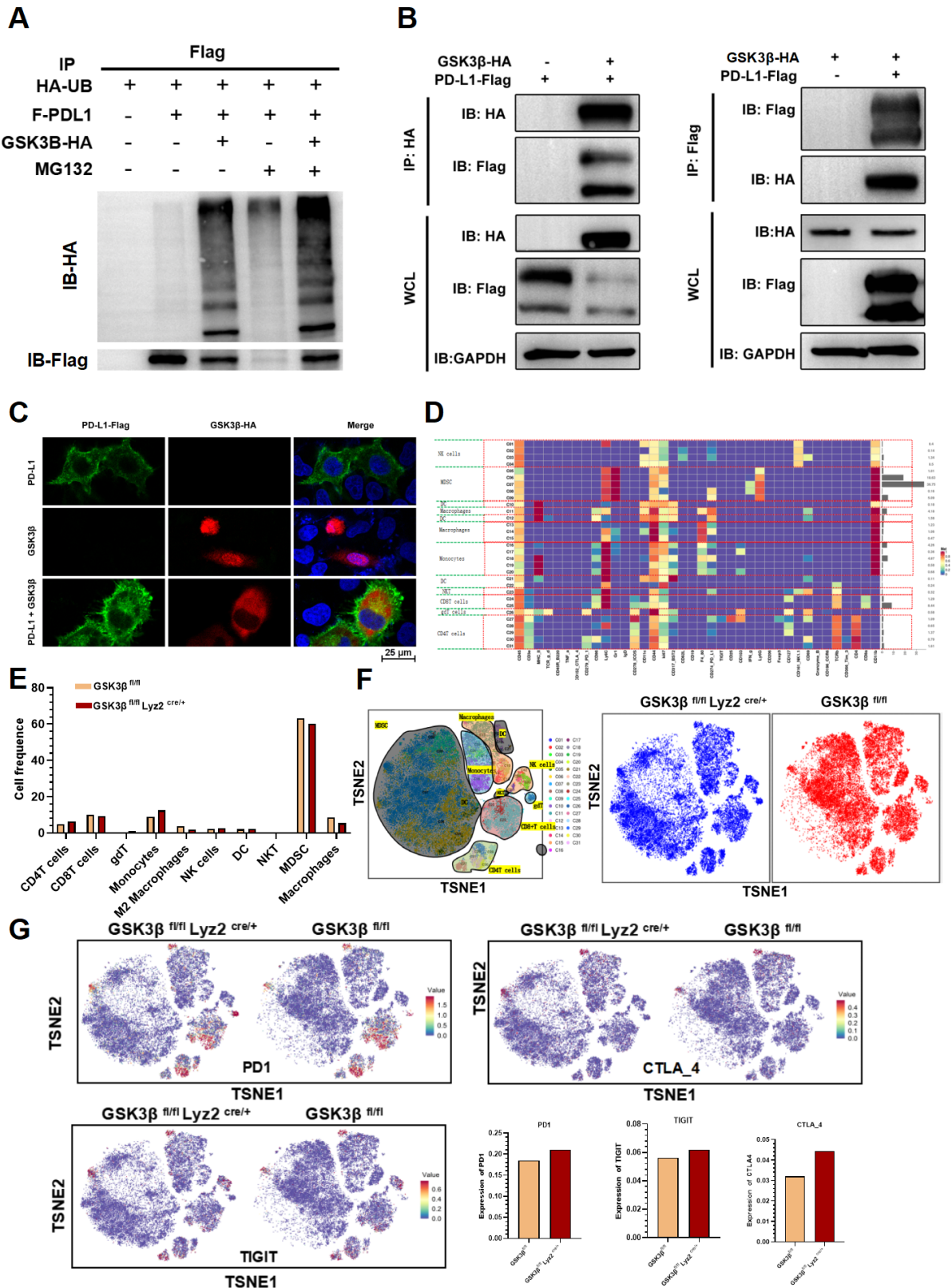


Figure 4 Macrophage GSK3 β deficiency enhanced the sensitivity of anti-PD1 immunotherapy for HCC by decreasing PD-L1 ubiquitination. (A) The ubiquitination expression of PD-L1 via co-immunoprecipitation. (B) Coimmunoprecipitation assays showed an interaction between GSK3 β and PD-L1 in 293 T cell. (C) Immunofluorescence staining assays of GSK3 β and PD-L1 in 293T cells observed by confocal microscopy. (D) There were 31 cell clusters in total, which were defined in the respective groups. (E) The histogram showing the number of the respective cell clusters in different groups by mass cytometry. (F) TSNE plot showing distribution of 31 cell clusters. (G) TSNE plot showing distribution of PD1, TIGIT and CTLA4 in two groups. The histogram showing the number of PD1+, TIGIT+ and CTLA4+ cell clusters in different groups. HCC, hepatocellular carcinoma; TSNE: t-distributed stochastic neighbor embedding; TIGIT: T cell immunoreceptor with Ig and ITIM domains.

$cre/+$ group compared with the $GSK3\beta^{fl/fl}$ group. On the contrary, NK and DC cells presented an upward trend (figure 4E). $CD8^+$ T cells failed to exhibit clear change (figure 4E). In addition, it was revealed that PD1, TIGIT, CTLA4 expressions elevated in $GSK3\beta^{fl/fl}$ $Lyz2^{cre/+}$ mice (figure 4G). Hence, $GSK3\beta$ deficiency in macrophages contributed to immune activation of HCC.

The sensitivity of anti-PD1 immunotherapy in HCC increased in $GSK3\beta^{fl/fl}$ $Lyz2^{cre/+}$ mice

The above experiments confirmed the relationship between $GSK3\beta$ and the primary resistance of anti-PD1 immunotherapy for HCC. Then, we further verify our result in $GSK3\beta^{fl/fl}$ $Lyz2^{cre/+}$ mice that knockdown the expression of $GSK3\beta$ in TAMs can enhance the sensitivity of anti-PD1 immunotherapy. We injected Hep1-6 cells in $GSK3\beta^{fl/fl}$ and $GSK3\beta^{fl/fl}$ $Lyz2^{cre/+}$ mice and treated the mice with PBS and anti-PD1 (figure 5A). Hep1-6 cells with anti-PD1 in $GSK3\beta^{fl/fl}$ grew faster in mice, which, however, slowed down in $GSK3\beta^{fl/fl}$ $Lyz2^{cre/+}$ anti-PD1 group (figure 5B). With the addition of anti-PD1 on the eighth day in $GSK3\beta^{fl/fl}$ $Lyz2^{cre/+}$ anti-PD1 group, the tumors tended to grow more slowly (figure 5B). After the mice were killed on day 20, $GSK3\beta^{fl/fl}$ $Lyz2^{cre/+}$ anti-PD1 group presented smaller tumor volume and weight relative to $GSK3\beta^{fl/fl}$ anti-PD1 group (figure 5C,D). According to the immunohistochemistry results, compared with the $GSK3\beta^{fl/fl}$ group, the PD1, PD-L1 and CD8 expressions elevated in $GSK3\beta^{fl/fl}$ $Lyz2^{cre/+}$ group, but Ki67 expression decreased (figure 5E,F). In the $GSK3\beta^{fl/fl}$ $Lyz2^{cre/+}$ anti-PD1 group, CD8 presented a higher expression but Ki67, PD-L1 and PD1 presented downregulation (figure 5E,F). The above evidence indicated that expression knockdown of $GSK3\beta$ in TAM assisted in enhancing the anti-HCC effect in combination with the anti-PD1 therapy in vivo.

The expression of $CD14^+GSK3\beta^+$ cells from PBMC can noninvasively predict anti-PD1 sensitivity in HCC patients

After summarizing the above experimental results, we considered whether the sensitivity to anti-PD1 immunotherapy of HCC patients can be predicted by detecting the content of $GSK3\beta$ in PBMCs. On that basis, nine blood samples with anti-PD1 pre-treatment were examined through mass spectrometry (three sensitive, six non-sensitive). We focused on cycling single intact $CD45^+$ immune cells with normal activity from selected cell masses (online supplemental figure S5). All samples presented clustering as well as subgroup annotation of $CD45^+$ immune cells. We obtained 32 cell clusters, and each cell cluster was defined by its specific marker (figure 6A,B, online supplemental figure S6). We analyzed the cell populations of anti-PD1 pretreatment sensitive (S, n=3 samples) and non-sensitive (NS, n=6 samples) patients and found that monocyte populations were significantly elevated in the insensitive group (figure 6C,D). In addition, we found that one monocyte cluster named $CD14^+GSK3\beta^+$ cells were

upregulated in NS group compared with S group (figure 6E). We expanded the sample size to further verify this conclusion. We extracted PBMCs from 10 sensitive and 9 insensitive anti-PD1 HCC patients for flow cytometry and found that the insensitive group had a higher percentage of $CD14^+GSK3\beta^+$ than the sensitive group (figure 6F,G). The above results suggested that $CD14^+GSK3\beta^+$ cell clusters in PBMC can predict anti-PD1 sensitivity of HCC patients.

Escitalopram added in TAMs upregulated PD-L1 expression by reducing $GSK3\beta$ and improved the anti-PD1 therapy sensitivity in HCC

We aimed at further translating above results into clinical practice. Our experiment in $GSK3\beta^{fl/fl}$ $Lyz2^{cre/+}$ mice proved that knockout of $GSK3\beta$ in TAMs can effectively inhibit HCC and sensitize anti-PD1 immunotherapy. Then can intraperitoneal injection of $GSK3\beta$ inhibitor in WT mice have the same effect? For addressing the possible effect exerted by $GSK3\beta$ inhibitor in HCC in vivo, Hep1-6 cells were subcutaneous injected in C57BL/6 mice that were treated with PBS, $GSK3\beta$ inhibitor, anti-PD1, as well as $GSK3\beta$ inhibitor+anti-PD1, respectively. Hep1-6 cells with PBS grew faster in mice, however, such trend was slowed down in $GSK3\beta$ inhibitor or anti-PD1 group (figure 7A). With the addition of anti-PD1 on the eighth day in $GSK3\beta$ inhibitor+anti-PD1 group, the tumors tended to grow more slowly (figure 7A). We sacrificed the mice on day 20, and found smaller tumor volume and weight in $GSK3\beta$ inhibitor or anti-PD1 group relative to PBS group, and smaller tumor volume and weight in $GSK3\beta$ inhibitor+anti-PD1 relative to $GSK3\beta$ inhibitor or anti-PD1 group (figure 7B,C). According to the immunohistochemistry results, relative to the PBS group, the injection of $GSK3\beta$ inhibitor led to increased PD1, PD-L1 and CD8 expressions, but decreased Ki67 expression (figure 7D,E). The $GSK3\beta$ inhibitor+anti-PD1 group presented a higher CD8 expression, but lower Ki67, PD-L1 and PD1 expressions (figure 7D,E). The above exciting results suggested that intraperitoneal injection of $GSK3\beta$ inhibitors can also inhibit HCC and sensitize anti-PD1 immunotherapy.

We have to investigate which drugs can play a role like $GSK3\beta$ inhibitors in the clinic since $GSK3\beta$ inhibitors have not been used in the clinic. Li *et al* pointed out that stimulating the release of 5-hydroxytryptamine (5-HT) and reducing its reuptake can increase phospho-Ser9- $GSK3\beta$ levels. While looking for the target transformation drug, we found that escitalopram could enhance the effect of 5-HT energy in the central nervous system, meanwhile inhibiting the reuptake of 5-HT.¹⁸ After further literature review, we found that escitalopram ameliorated cognitive impairments, selectively attenuating the phosphorylated tau accumulation in the stressed rats by adjusting hypothalamic–pituitary–adrenal axis activity as well as the insulin receptor substrate/ $GSK3\beta$ signaling pathway.¹⁹ Accordingly, we aimed to explore whether escitalopram can be adopted to replace the effects of $GSK3\beta$ inhibitors given that escitalopram is already well-established

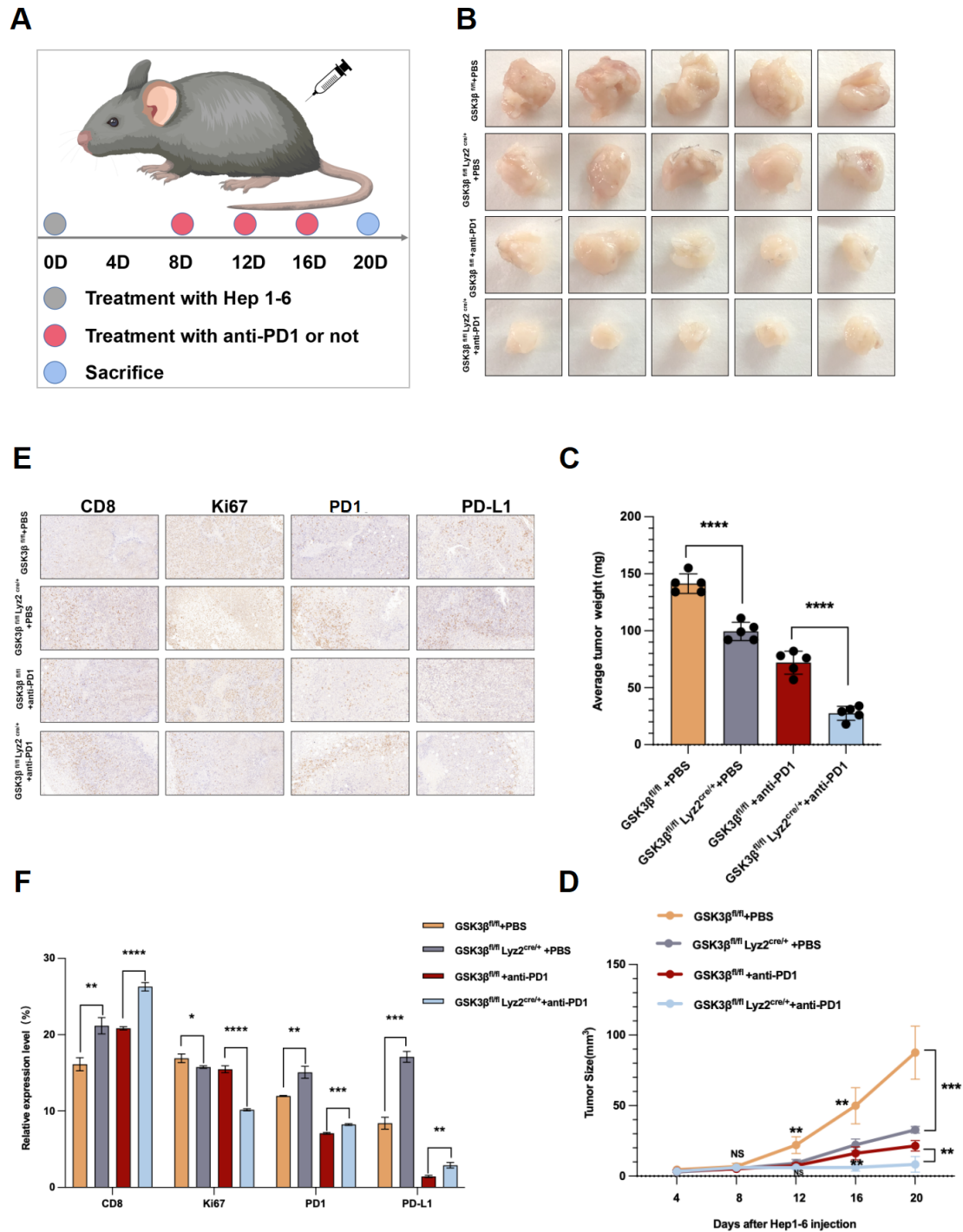


Figure 5 The sensitivity of anti-PD1 immunotherapy in HCC was increased in GSK3β^{fl/fl} Lyz2^{cre/+} mice. (A) Schematic diagram of establishment of mouse subcutaneous tumor model in each group. (B) Images of subcutaneous tumors in each group. (C, D) Analysis of subcutaneous tumors in the respective groups. (E, F) Immunohistochemistry results of CD8, Ki67, PD-L1 and PD1 expression in the respective groups. *p<0.05, **p<0.01, ***p<0.001, ****p<0.0001. ns indicated no significant different. HCC, hepatocellular carcinoma.

clinical drugs. We attempted to use escitalopram to test its therapeutic potential against HCC (online supplemental figure S7A). The western blotting assisted in validating the expression of proteins and results revealed that when escitalopram was added in TAMs, GSK3β was downregulated while GSK3β ser9 was upregulated, indicating the activity of GSK3β was significantly inhibited,

and PD-L1 was upregulated (online supplemental figure S7B). qRT-PCR results showed that escitalopram group exhibited considerably lower CD206, CD163, ARG1 of M2 phenotype expressions relative to the control group (online supplemental figure S7C). We also explored the effect of escitalopram treated TAM on tumorigenesis and development through a series of experiments. The results

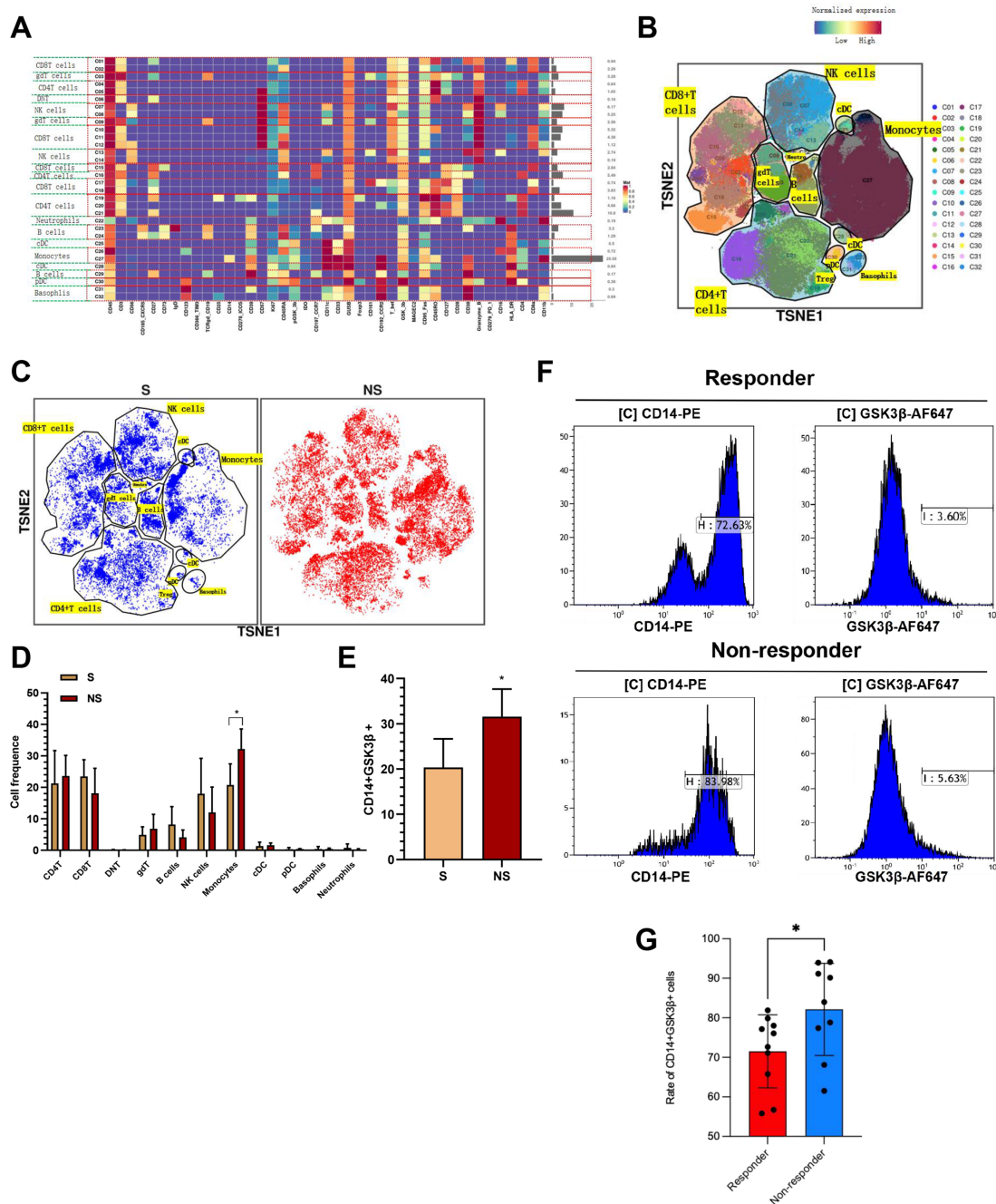


Figure 6 The expression of CD14⁺GSK3β⁺ cells from PBMC could noninvasively predict anti-PD1 sensitivity in HCC patients. (A) There were 32 cell clusters in total, which were defined in the respective groups. (B) TSNE plot showing distribution of 32 cell clusters. (C) TSNE diagram showing distribution of cell clusters in the anti-PD1 sensitive and non-sensitive group samples. (D) The histogram showing the number of the respective cell clusters in the anti-PD1 sensitive and non-sensitive groups by mass cytometry. (E) The histogram showing the expression of CD14⁺GSK3β⁺ cell in the anti-PD1 sensitive and non-sensitive groups. (F–G) PBMCs were collected from 10 sensitive and 9 insensitive anti-PD1 HCC patients, and the expression of CD14 and GSK3β was measured by flow cytometry. **p* < 0.05. HCC, hepatocellular carcinoma; PBMC, peripheral blood mononuclear cell.

showed that TAMs significantly inhibited HCC cells in escitalopram group compared with control group (online supplemental figure S7D–G).

Whether escitalopram is capable of inhibiting tumor as well as enhancing anti-PD1 sensitivity *in vivo* shall be investigated in depth. Hence, we injected Hep1-6 cells in C57BL/6 mice, and treated the mice with PBS, escitalopram, anti-PD1, and escitalopram+anti-PD1. Hep1-6

cells with PBS grew faster in mice, while the trend slowed down in escitalopram or anti-PD1 group (figure 7F). After adding anti-PD1 on the eighth day in escitalopram+anti-PD1 group, the tumors tended to grow more slowly (figure 7F). We killed the mice on day 20, finding smaller tumor volume and weight in escitalopram or anti-PD1 group relative to PBS group, and smaller tumor volume and weight in escitalopram+anti-PD1 relative

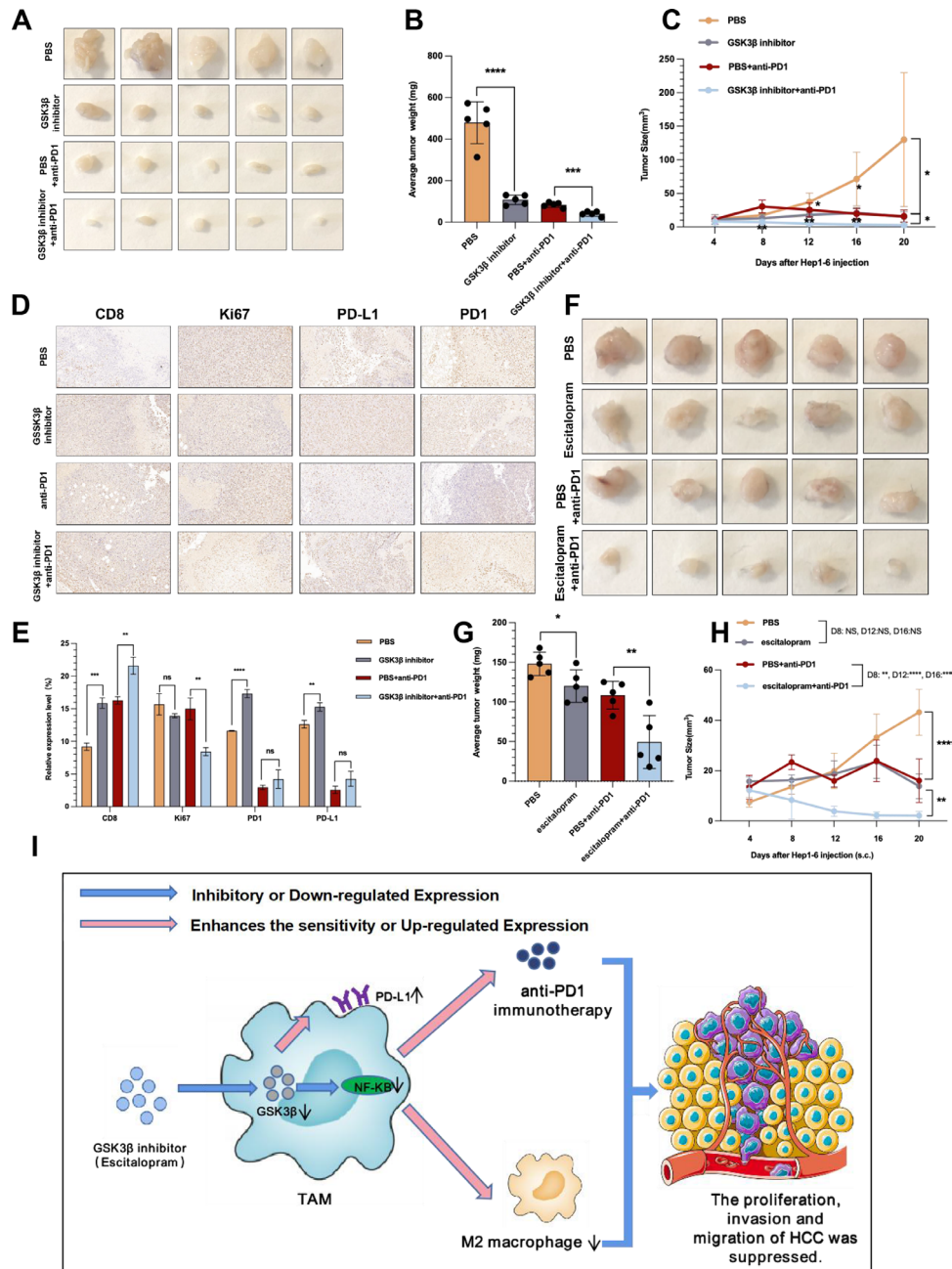


Figure 7 Escitalopram reduced tumor growth in mice and increased the efficacy of anti-PD1 treatment against HCC. (A) Images of subcutaneous tumors in each group (PBS, GSK3 β inhibitor, anti-PD1, GSK3 β inhibitor+ anti-PD1). (B, C) Analysis of subcutaneous tumors in the respective groups. (D, E) Immunohistochemistry results of CD8, Ki67, PD-L1 and PD1 expression in the respective groups. (F) Images of subcutaneous tumors in each group (PBS, escitalopram, anti-PD1, and escitalopram+anti-PD1). (G, H) Analysis of subcutaneous tumors in the respective groups. (I) Pattern diagram showing that macrophage GSK3 β deficiency inhibits the development of HCC and enhances the sensitivity of anti-PD1 immunotherapy. * $p < 0.05$, ** $p < 0.01$, *** $p < 0.001$. **** $p < 0.0001$. ns indicated no significant different. HCC, hepatocellular carcinoma; PBS, phosphate buffered saline; TAM, tumor-associated macrophage.

to escitalopram or anti-PD1 group (figure 7G,H). The above evidence suggested that escitalopram, in combination with the anti-PD1 treatment in vivo, was capable of enhancing the anti-HCC effect.

DISCUSSION

Tumor immunotherapy, such as PD1/PD-L1 mAbs, has brought new light to the treatment of tumor patients.

Compared with traditional molecular targeted therapy and chemotherapy, immunotherapy has a high incidence of drug resistance, preventing a huge group of tumor patients from benefiting from it, and becoming the most severe test for immunotherapy.²⁰ Resistance to PD1/PD-L1 antibodies is related to a variety of tumor cytokines, tumor metabolic pathways, etc.²¹ In existing research, resistance was separated into secondary resistance and

primary resistance in accordance with the emergence of resistance. Secondary resistance is the initial use of PD1/PD-L1 mAb with significant effect, and then with the deepening of treatment, drug resistance appears. Primary resistance, on the other hand, is the ineffective treatment of initial immunotherapy.²² Existing research has confirmed that the emergence of related drug resistance is most directly related to the PD1/PD-L1 expression on the cell surface, and other related factors include loss of primary and costimulatory signals, tumor micro-environment as well as epigenetic modifications.²⁰ The study found that TAM-GSK3 β cell cluster was upregulated in non-responders of anti-PD1 therapy in HCC based on scRNA-seq and immunofluorescence, thus finding new therapeutic targets for the anti-PD1 treatment in HCC.

GSK3 β , a kinase that regulates multiple metabolic pathways and cell growth signals, has been considered a promising target for cancer therapy. The role played by GSK3 β in the regulation of metastasis, invasion, tumor growth, DNA repair, cell cycle, and apoptosis reveals the therapeutic relationship of such target, meanwhile providing the basic principle for drug combinations. Moreover, new data about GSK3 β serving for mediating the anticancer immune response emphasize the possible clinical uses of new selective GSK3 β inhibitors involved in clinical research.²³ The publications over the past few years have stressed the role played by GSK3 β in the regulation of the immune response. Taylor *et al* investigated the way GSK3 β inhibition downregulated PD1 on T cells. GSK3 β inhibition reduced tumor growth as well as metastasis through the downregulation of PD1 on CD8⁺ T cells in the melanoma model, but minimally affecting NK cells without significantly impacting CD4⁺ T cells. GSK-3 α/β inhibitor can reduce the transcription and expression levels of PD1, and can achieve similar antitumor effects as anti-PD1 and PD-L1 blocking antibodies, including B16 melanoma or EL4 lymphoma. In addition, genetic defects of GSK3 α/β can inhibit PD1 expression on CD8+T cells, thereby limiting tumor metastasis.²⁴ Besides its critical role in PD1 pathway, a breast cancer study proved the possible role played by GSK3 β in PD-L1 pathway.²⁵ Specific as follows: PARP inhibitors are capable of upregulating the PD-L1 expression in BC cell lines and animal models. Mechanistically, PARP inhibitors attenuate GSK3 β activity, thereby enhancing PARP inhibitor-mediated upregulation of PD-L1. This series of reactions re-sensitizes cancer cells to T-cell killing, thereby weakening anticancer immunity. The efficacy of PARP inhibitor combined with anti-PD-L1 therapy showed an obvious improvement in vivo relative to drug alone. The above published studies fully demonstrate that GSK3 β greatly regulates PD1/PD-L1-related pathways. This undoubtedly provides inspiration for our experimental design. In our study, when GSK3 β was knocked out in myeloid, PD1 and PD-L1 increased simultaneously. This is inconsistent with the conclusion drawn in previous studies, that is, previous studies have proved that when GSK3 β is down regulated, the expression level of PD1 decreases. We have to think about the

reasons for this result. First, we measured the expression of PD1 on the whole sample, not on the surface of CD8 T cells involved in other articles. Second, the total number of CD8 T cells increases after the myeloidknocks out GSK3 β , so the number of PD1 positive CD8 T cells also elevates, leading to this result. But this does not affect the effect of anti immunotherapy. In addition, GSK3 β over-expression weakened NK cell ability to eliminate acute myelocytic leukemia (AML) cells, but GSK3 β inhibition strengthened NK cell cytotoxic activity in human AML mouse models.²⁶ Our experiment innovatively focused on the differential expression of GSK3 β in HCC TAM, illustrating the role of GSK3 β in fighting HCC from a new perspective. We found for the first time that inhibition of GSK3 β upregulated PD-L1 expression by inhibiting its ubiquitination. GSK3 β inhibitor enhanced the anti-PD1 immunotherapy sensitivity in HCC in vivo, thus making the study on GSK3 β and tumor immunity take on a greater significance.

Mass spectrometry enables precise immunotyping of cell populations, all-sided analysis of intracellular signaling networks, analysis of functional connections between cell subpopulations, as well as the high-throughput multiparameter detection of large numbers of samples.^{27 28} The study detected two tumor samples from GSK3 β ^{fl/fl} and GSK3 β ^{fl/fl} Lyz2^{cre/+} mice through mass spectrometry, respectively. As found, the relative proportion of M2 macrophages, macrophages, MDSC, Tregs in GSK3 β ^{fl/fl} Lyz2^{cre/+} group declined continuously relative to the GSK3 β ^{fl/fl} group, whereas DC and NK cells elevated. CD8⁺ T cells did not change significantly, perhaps because the sample size was too small or CD8⁺ T groups were not classified in detail, but immunohistochemical results confirmed that CD8⁺ T increased in GSK3 β ^{fl/fl} Lyz2^{cre/+} group. The comprehensive analysis of how GSK3 β knockout in macrophages affects tumor immune microenvironment is reported for the first time in the world. In general, GSK3 β knockout in macrophages can inhibit immunosuppressive cells, especially myeloid cells. In addition, nine blood samples with anti-PD1 pretreatment were examined through mass spectrometry (three sensitive, six non-sensitive). The result showed that the insensitive group possessed higher proportion of monocytes from PBMC relative to the sensitive group, while other cells, such as CD8⁺ T cells, showed no significant difference. Based on the flow validation with an enlarged sample size, we found that the insensitive group had a higher percentage of CD14⁺GSK3 β ⁺ than the sensitive group. Based on existing research, accumulated immature myeloid cells in tumor microenvironment are capable of suppressing antitumor immune responses as well as promoting tumor growth. MDSCs from human PBMCs cocultured with SK-MEL-5 cancer cells in vitro can significantly inhibit CD8⁺ T cell proliferation as well as IFN secretion, and ILT3 antibody can reverse the above process.²⁹ Thus, it may be necessary to use a significantly larger sample size to verify more accurate results.

The anti-HCC effect of the antidepressant escitalopram and its ability to enhance the sensitivity of anti-PD1 therapy make us a bright sight. Wang *et al* confirmed that Monoamine oxidase A (MAO-A), a kind of enzyme with an excellent function in the brain, can break down neurotransmitters and then have an effect on mood and behavior, restraining antitumor T cell immunity by adjusting intratumoral T cell autocrine serotonin signaling. In general, the above data suggested MAO-A as an immune checkpoint and recommended to repurpose MAO antidepressants in the cancer immunotherapy.³⁰ This result was consistent with ours. We suggest that antidepressant escitalopram can be used as anti-PD1 sensitizers, especially in HCC patients with cold tumors, which needs to be verified by further clinical trials.

There are some limitations in this study. In our study, we were surprised to find out that the GSK3 β inhibitor had much stronger anticancer effect than GSK3 β deficiency in macrophage in mouse experiment. This surprising and exciting result got us thinking. We discussed and analyzed the possible causes. The dose of GSK3 β inhibitor injected intraperitoneally, drug toxicity, and individual differences in mice may be the underlying reasons. Second, GSK3 β expression on other cells, such as immune cells or cancer cells, may be associated with cancer suppression. In future further studies, this will serve as a new entry point to explore the potential of this target against HCC. In addition, there are other shortcomings in this study. First, we clarified reduction of GSK3 β in TAMs significantly upregulated PD-L1 expression by inhibiting its ubiquitination in HCC, but did not clarify the specific site. Li *et al* reported that MET phosphorylated and activated GSK3 β at tyrosine 56, thus downregulating PD-L1 expression by liver cancer cells.³¹ Wu *et al* suggested that WSX1 could suppress tumor without relying on IL-27, primarily dependent on CD8 T-cell immune surveillance through the downregulation of neoplastic PD-L1 expression and the relevant CD8 T-cell exhaustion in HCC. From the mechanistical perspective, WSX1 reduces an isoform of PI3K-PI3K δ transcriptionally and then makes AKT inactive, which limits the GSK3 β inhibition induced by AKT. Subsequently, activated GSK3 β promotes PD-L1 to be degraded and reduces PD-L1.³² In-depth studies shall be conducted to investigate the regulation function possessed by GSK3 β and PD-L1 in TAMs. Second, the number of clinical samples in this study was small due to the high risk of massive bleeding in the puncture operation of HCC patients before anti-PD1 treatment. We look forward to more data before and after anti-PD1 treatment in HCC to support the view of this study. Third, we did not use more models (eg, patient-derived xenografts (PDX) model) for verifying the conclusions of this study due to limited scientific research funds. Finally, this study didn't identify the site where escitalopram inhibited the activity of GSK3 β , but only preliminarily verified its function, which will be further explored in our future study.

CONCLUSION

Briefly, macrophage GSK3 β deficiency inhibits the development of HCC by inhibiting the M2 phenotype of TAMs as well as strengthens the anti-PD1 immunotherapy sensitivity for HCC by decreasing PD-L1 ubiquitination (figure 7I). The expression of CD14⁺GSK3 β ⁺ cell cluster in peripheral blood can noninvasively predict anti-PD1 sensitivity in HCC patients. This study provides novel strategies and methods to predict anti-PD1 sensitivity and increase anti-PD1 therapeutic effect, and brings new hope for HCC patients.

Author affiliations

¹Hepatobiliary/Liver Transplantation Center, The First Affiliated Hospital of Nanjing Medical University, Key Laboratory of Living Donor Transplantation, Chinese Academy of Medical Sciences, Nanjing, Jiangsu, China

²Department of General Surgery, Nanjing First Hospital, Nanjing Medical University, Nanjing, Jiangsu, China

³Jiangsu Key Laboratory of Infection and Immunity, Institute of Biology and Medical Sciences, Soochow University, Suzhou, Jiangsu, China, Suzhou, Jiangsu, China

⁴Zhejiang Puluoting Health Technology Co., Ltd, Hangzhou, Zhejiang, China

⁵First Teaching Hospital of Tianjin University of Traditional Chinese Medicine, Tianjin, China

⁶State Key Laboratory of Modern Chinese Medicine, Tianjin University of Traditional Chinese Medicine, Tianjin, China

Acknowledgements We express our sincere appreciation to the National Natural Science Foundation of China (No.82070676) and the National Natural Science Key Foundation of China(No.31930020) for the grants.

Contributors There are four first authors in the manuscript who made equal contribution to the project. WW T is responsible for the overall content as the guarantor. GS S, HY L, J Z and JY Z took charge of experiment design and performance. T H, GQ S, HS C, DW R, XY K, ZH Z and QH J carried out part of experiment. Besides, we have four corresponding authors. L L, WW T, XH W and YX X completed the data interpretation, and the manuscript editing and revision. WW T, XH W, and YX X designed the study and critically revised the manuscript. The final manuscript has been read by and obtained the approval of all authors.

Competing interests None declared.

Patient consent for publication Not applicable.

Ethics approval Patients were informed about the information with respect to the study following Declaration of Helsinki. We collected HCC cancer tissues and blood from HCC patients undergoing surgical treatment from the First Affiliated Hospital of Nanjing Medical University, as well as obtained participants' informed consent. This study involves human participants and has obtained the approval of the Ethics Committee of above university. The approved ID number is 2019-SRFA-238.

Provenance and peer review Not commissioned; externally peer reviewed.

Data availability statement All data relevant to the study are included in the article or uploaded as online supplemental information.

Supplemental material This content has been supplied by the author(s). It has not been vetted by BMJ Publishing Group Limited (BMJ) and may not have been peer-reviewed. Any opinions or recommendations discussed are solely those of the author(s) and are not endorsed by BMJ. BMJ disclaims all liability and responsibility arising from any reliance placed on the content. Where the content includes any translated material, BMJ does not warrant the accuracy and reliability of the translations (including but not limited to local regulations, clinical guidelines, terminology, drug names and drug dosages), and is not responsible for any error and/or omissions arising from translation and adaptation or otherwise.

Open access This is an open access article distributed in accordance with the Creative Commons Attribution Non Commercial (CC BY-NC 4.0) license, which permits others to distribute, remix, adapt, build upon this work non-commercially, and license their derivative works on different terms, provided the original work is properly cited, appropriate credit is given, any changes made indicated, and the use is non-commercial. See <http://creativecommons.org/licenses/by-nc/4.0/>.

ORCID iDs

Siqi Zhao <http://orcid.org/0000-0002-3678-7912>Weiwei Tang <http://orcid.org/0000-0002-8516-819X>Yongxiang Xia <http://orcid.org/0000-0001-6589-797X>

REFERENCES

- 1 Bruix J, Qin S, Merle P, et al. Regorafenib for patients with hepatocellular carcinoma who progressed on sorafenib treatment (RESORCE): a randomised, double-blind, placebo-controlled, phase 3 trial. *Lancet* 2017;389:56–66.
- 2 Kudo M, Finn RS, Qin S, et al. Lenvatinib versus sorafenib in first-line treatment of patients with unresectable hepatocellular carcinoma: a randomised phase 3 non-inferiority trial. *Lancet* 2018;391:1163–73.
- 3 Lencioni R, Chen X-P, Dagher L, et al. Treatment of intermediate/advanced hepatocellular carcinoma in the clinic: how can outcomes be improved? *Oncologist* 2010;15 Suppl 4:42–52.
- 4 Motzer RJ, Escudier B, McDermott DF, et al. Nivolumab versus everolimus in advanced renal-cell carcinoma. *N Engl J Med* 2015;373:1803–13.
- 5 Herbst RS, Baas P, Kim D-W, et al. Pembrolizumab versus docetaxel for previously treated, PD-L1-positive, advanced non-small-cell lung cancer (KEYNOTE-010): a randomised controlled trial. *Lancet* 2016;387:1540–50.
- 6 Postow MA, Chesney J, Pavlick AC, et al. Nivolumab and ipilimumab versus ipilimumab in untreated melanoma. *N Engl J Med* 2015;372:2006–17.
- 7 El-Khoueiry AB, Sangro B, Yau T, et al. Nivolumab in patients with advanced hepatocellular carcinoma (CheckMate 040): an open-label, non-comparative, phase 1/2 dose escalation and expansion trial. *Lancet* 2017;389:2492–502.
- 8 Bartoschek M, Oskolkov N, Bocci M, et al. Spatially and functionally distinct subclasses of breast cancer-associated fibroblasts revealed by single cell RNA sequencing. *Nat Commun* 2018;9:1–13.
- 9 Savas P, Virassamy B, Ye C, et al. Single-Cell profiling of breast cancer T cells reveals a tissue-resident memory subset associated with improved prognosis. *Nat Med* 2018;24:986–93.
- 10 Beurel E, Grieco SF, Jope RS. Glycogen synthase kinase-3 (GSK3): regulation, actions, and diseases. *Pharmacol Ther* 2015;148:114–31.
- 11 Murata M. Inflammation and cancer. *Environ Health Prev Med* 2018;23:1–8.
- 12 Li C, Xue VW, Wang Q-M, et al. The Mincle/Syk/NF- κ B signaling circuit is essential for maintaining the Protumoral activities of tumor-associated macrophages. *Cancer Immunol Res* 2020;8:1004–17.
- 13 Zhou H, Wang H, Ni M, et al. Glycogen synthase kinase 3 β promotes liver innate immune activation by restraining AMP-activated protein kinase activation. *J Hepatol* 2018;69:99–109.
- 14 Xia Y, Zhuo H, Lu Y, et al. Glycogen synthase kinase 3 β inhibition promotes human iTreg differentiation and suppressive function. *Immunol Res* 2015;62:60–70.
- 15 Li J, Gao J, Zhou H, et al. Inhibition of glycogen synthase kinase 3 β increases the proportion and suppressive function of CD19+CD24hiCD27+ Breg cells. *Front Immunol* 2020;11:3119.
- 16 Xia Y, Rao J, Yao A, et al. Lithium exacerbates hepatic ischemia/reperfusion injury by inhibiting GSK-3 β /NF- κ B-mediated protective signaling in mice. *Eur J Pharmacol* 2012;697:117–25.
- 17 Li C-W, Lim S-O, Xia W, et al. Glycosylation and stabilization of programmed death ligand-1 suppresses T-cell activity. *Nat Commun* 2016;7:1–11.
- 18 Li X, Zhu W, Roh M-S, et al. In vivo regulation of glycogen synthase kinase-3beta (GSK3beta) by serotonergic activity in mouse brain. *Neuropsychopharmacology* 2004;29:1426–31.
- 19 Wu C, Gong W-G, Wang Y-J, et al. Escitalopram alleviates stress-induced Alzheimer's disease-like tau pathologies and cognitive deficits by reducing hypothalamic-pituitary-adrenal axis reactivity and insulin/GSK-3 β signal pathway activity. *Neurobiol Aging* 2018;67:137–47.
- 20 Sharma P, Allison JP. The future of immune checkpoint therapy. *Science* 2015;348:56–61.
- 21 Li Z, Sun G, Sun G, et al. Various uses of PD1/PD-L1 inhibitor in oncology: opportunities and challenges. *Front Oncol* 2021;11:771335.
- 22 Kreiter S, Vormehr M, van de Roemer N, et al. Mutant MHC class II epitopes drive therapeutic immune responses to cancer. *Nature* 2015;520:692–6.
- 23 Sahin I, Eturi A, De Souza A, et al. Glycogen synthase kinase-3 beta inhibitors as novel cancer treatments and modulators of antitumor immune responses. *Cancer Biol Ther* 2019;20:1047–56.
- 24 Taylor A, Rothstein D, Rudd CE. Small-molecule inhibition of PD-1 transcription is an effective alternative to antibody blockade in cancer therapy. *Cancer Res* 2018;78:706–17.
- 25 Jiao S, Xia W, Yamaguchi H, et al. PARP inhibitor upregulates PD-L1 expression and enhances cancer-associated immunosuppression. *Clin Cancer Res* 2017;23:3711–20.
- 26 Parameswaran R, Ramakrishnan P, Moreton SA, et al. Repression of GSK3 restores NK cell cytotoxicity in AML patients. *Nat Commun* 2016;7:1–11.
- 27 Devine RD, Behbehani GK. Mass cytometry, imaging mass cytometry, and multiplexed ion beam imaging use in a clinical setting. *Clin Lab Med* 2021;41:297–308.
- 28 Maby P, Corneau A, Galon J. Phenotyping of tumor infiltrating immune cells using mass-cytometry (CyTOF). *Methods Enzymol* 2020;632:339–68.
- 29 Singh L, Muise ES, Bhattacharya A, et al. ILT3 (LILRB4) promotes the immunosuppressive function of tumor-educated human monocytic myeloid-derived suppressor cells. *Mol Cancer Res* 2021;19:702–16.
- 30 Wang X, Li B, Kim YJ, et al. Targeting monoamine oxidase A for T cell-based cancer immunotherapy. *Sci Immunol* 2021;6:p. eabh2383.
- 31 Li H, Li C-W, Li X, et al. MET inhibitors promote liver tumor evasion of the immune response by stabilizing PDL1. *Gastroenterology* 2019;156:1849–61.
- 32 Wu M, Xia X, Hu J, et al. WSX1 act as a tumor suppressor in hepatocellular carcinoma by downregulating neoplastic PD-L1 expression. *Nat Commun* 2021;12:1–16.